New methods of testing Lorentz violation in electrodynamics

Michael E. Tobar¹, Peter Wolf^{2,3}, Alison Fowler¹, John G. Hartnett¹

¹University of Western Australia, School of Physics, Nedlands 6907 WA, Australia ²BNM-SYRTE, Observatoire de Paris, 61 Av. de l'Observatoire, 75014 Paris, France ³Bureau International des Poids et Mesures, Pavillon de Breteuil, 92312 Se`vres CEDEX, France

We investigate experiments that are sensitive to the scalar and parity-odd coefficients for Lorentz violation in the photon sector of the Standard Model Extension (SME). Of the classic tests of special relativity, Ives-Stilwell (IS) experiments are shown to be sensitive to the scalar coefficient, but at only parts in 10^4 . We then propose asymmetric Mach-Zehnder interferometers with different electromagnetic properties in the two arms. A recycling technique based on an travelling wave resonator is also proposed to improve the sensitivity. Based on these proposals we estimate that with present technology, measurements of the scalar and parity odd coefficients should be possible at parts in 10^{11} and 10^{15} respectively.

I. INTRODUCTION

The postulate of Lorentz Invariance (LI) is at the heart of special and general relativity and therefore one of the cornerstones of modern physics. The central importance of this postulate has motivated tremendous work to experimentally test LI with ever increasing precision ¹. Additionally, many unification theories (e.g. string theory or loop gravity) are expected to violate LI at some level ²⁻⁴, which further motivates experimental searches for such violations.

Numerous test theories that allow the modelling and interpretation of experiments that test LI have been developed. Kinematical frameworks^{5, 6} postulate a simple parameterisation of the Lorentz transformations with experiments setting limits on the deviation of those parameters from their special relativistic values. A more fundamental approach is offered by theories that parameterize the coupling between gravitational and non-gravitational fields $TH_{\epsilon\mu}^{1,7}$ (or χ_g formalisms). Formalisms based on string theory ^{2, 3} have the advantage of being well motivated by theories of physics that are at present good candidates for a unification of gravity and the other fundamental forces of nature. Fairly recently a general Lorentz violating extension of the standard model of particle physics (Standard Model Extension, SME) has been developed ⁸⁻¹⁰ whose Lagrangian includes all parameterised Lorentz violating terms that can be formed from known fields. Many of the theories mentioned above are included as special cases of the SME ¹¹.

In this paper we restrict our attention to the photon sector of the SME. Within this restricted framework we analyse present and past experiments that can be shown to set limits on SME parameters that have not been determined previously, and propose new experiments that could significantly improve those limits.

As shown in ¹¹ the photon sector of the SME can be expressed in the form of modified source free Maxwell equations, which take their familiar form

$$\nabla . D = 0$$
 (1a)

$$\nabla . \mathbf{B} = 0 \tag{1b}$$

$$\nabla \times \mathbf{E} + \frac{\partial \mathbf{B}}{\partial t} = 0 \tag{1c}$$

$$\nabla \times \boldsymbol{H} - \partial \boldsymbol{D} /_{\partial t} = 0 \tag{1d}$$

but with modified definitions of **D** and **H**

$$\begin{bmatrix} \boldsymbol{D} \\ \boldsymbol{H} \end{bmatrix} = \begin{bmatrix} \varepsilon_0 (\ddot{\varepsilon}_r + \kappa_{DE}) & \sqrt{\frac{\varepsilon_0}{\mu_0}} \kappa_{DB} \\ \sqrt{\frac{\varepsilon_0}{\mu_0}} \kappa_{HE} & \mu_0^{-1} (\ddot{\mu}_r^{-1} + \kappa_{HB}) \end{bmatrix} \begin{bmatrix} \boldsymbol{E} \\ \boldsymbol{B} \end{bmatrix}$$
 (2)

Here κ_{DE} , κ_{DB} , κ_{HE} and κ_{HB} are all 3 x 3 matrices, which parameterize possible Lorentz violating terms as described in ¹¹. If we suppose the medium of interest has general magnetic or dielectric properties, then $\ddot{\varepsilon}_r$ and $\ddot{\mu}_r$ are also 3 x 3 matrices. In vacuum $\ddot{\varepsilon}_r$ and $\ddot{\mu}_r$ are identity matrices. For experimental tests it is convenient to further define linear combinations of the κ coefficients

$$(\widetilde{\kappa}_{e+})^{jk} = \frac{1}{2} (\kappa_{DE} + \kappa_{HB})^{jk},$$

$$(\widetilde{\kappa}_{e-})^{jk} = \frac{1}{2} (\kappa_{DE} - \kappa_{HB})^{jk} - \frac{1}{3} \delta^{kj} (\kappa_{DE})^{ll},$$

$$(\widetilde{\kappa}_{o+})^{jk} = \frac{1}{2} (\kappa_{DB} + \kappa_{HE})^{jk},$$

$$(\widetilde{\kappa}_{o-})^{jk} = \frac{1}{2} (\kappa_{DB} - \kappa_{HE})^{jk},$$

$$(\widetilde{\kappa}_{o-})^{jk} = \frac{1}{2} (\kappa_{DE} - \kappa_{HE})^{jk},$$

$$(3)$$

The first four of these equations define traceless 3 x 3 matrices, while the last defines a single coefficient. All $\widetilde{\kappa}$ matrices are symmetric except $\widetilde{\kappa}_{o+}$ which is antisymmetric (odd parity). These characteristics leave a total of 19 independent coefficients of the $\widetilde{\kappa}$ which are generally used to quote and compare experimental results ¹¹⁻¹⁵.

The κ tensors in (2) and (3) are frame dependent and consequently vary as a function of the co-ordinate system chosen to analyse a given experiment. In principle they may be constant and non-zero in any frame (e.g. the lab frame). However, any non-zero values are expected to arise from Planck-scale effects in the early Universe. Therefore the components of κ should be constant in a cosmological frame (e.g. the one defined by the CMB radiation) or any frame that moves with a constant velocity and shows no rotation with respect to the cosmological one. Consequently the conventionally chosen frame to analyze and compare experiments in the SME is a sun-centred, non-rotating frame as defined in ¹¹. The general procedure is to express the experimental observables in terms of the κ tensors in a suitably chosen experimental frame (e.g. the lab frame) and then to transform the κ tensors to the conventional sun-centred frame. This transformation will

introduce a time variation of the observables related to the movement of the experiment with respect to the sun-centred frame (typically introducing time variations of sidereal and semi-sidereal periods for an Earth fixed experiment).

So far two types of experiments have been used to set limits on 17 of the 19 independent components of $\widetilde{\kappa}$. Polarization measurements of light from distant astrophysical sources have been used to constrain all 10 independent components of $\widetilde{\kappa}_{e^+}$ and $\widetilde{\kappa}_{o^-}$ to less than 2 × 10^{-32} 11 , 12 . Modern versions of classical tests of special relativity (Michelson-Morley and Kennedy-Thorndike experiments) using optical 16 or microwave 13 , 15 , 17 cavities have recently constrained 4 components of $\widetilde{\kappa}_{e^-}$ to a few parts in 10^{-15} 15 and all three independent components of $\widetilde{\kappa}_{o^+}$ to a few parts in 10^{-11} 15 . For the time being, this leaves two parameters undetermined, $\widetilde{\kappa}_{e^-}^{ZZ}$ and $\widetilde{\kappa}_{t^*}$.

All cavity experiments $^{13, 15, 16}$ were fixed in the lab and therefore their orientation in the sun-centred frame varied only with the rotation of the Earth. This induces symmetry with respect to the Earth's rotation axis, which makes these experiments insensitive to $\widetilde{\kappa}_{e^-}^{ZZ}$. New cavity experiments that rotate in the lab are under way 18 and are expected to measure all 5 independent components of $\widetilde{\kappa}_{e^-}$ (including $\widetilde{\kappa}_{e^-}^{ZZ}$) with an uncertainty of 10^{-16} or less.

This will then leave only $\widetilde{\kappa}_{tr}$ undetermined. Experiments that are sensitive to that parameter are inherently difficult as $\widetilde{\kappa}_{tr}$ characterises the isotropic part of κ_{DE} and κ_{HB} in the sun centred frame, so any change in orientation of the experiment does not affect the $\widetilde{\kappa}_{tr}$ dependence of the observables. Therefore, modulation of the $\widetilde{\kappa}_{tr}$ dependence arises only from boost terms, i.e. from terms that contribute to $\widetilde{\kappa}_{tr}$ via the velocity of the experiment in the sun-centred frame. In this paper we examine existing experiments showing that such a mechanism can indeed lead to a sensitivity to $\widetilde{\kappa}_{tr}$, and propose new experiments that could determine $\widetilde{\kappa}_{tr}$ at a level of 10^{-11} .

In section II we analyse existing Lorentz invariance tests and identify a class of experiments that turn out to be sensitive to $\tilde{\kappa}_{tr}$. We explicitly model one of those experiments (at present, the most sensitive one) in the SME and derive an order of magnitude estimate for the limit that experiment sets on $\tilde{\kappa}_{tr}$. In section III we propose new interferometric experiments and estimate their sensitivity to $\tilde{\kappa}_{tr}$ and $\tilde{\kappa}_{0+}$. We show that such experiments should improve on the limit of $\tilde{\kappa}_{tr}$ derived in section II by several orders of magnitude. We summarise our results and conclude in section IV.

Throughout this paper we concentrate on the as-yet-undetermined photon SME parameter $\widetilde{\kappa}_{tr}$, and where appropriate the components of the odd parity tensor $\widetilde{\kappa}_{0+}$. Consequently, we assume that the matter sector of the SME conforms to Lorentz symmetry. Also, we will discuss sensitivities to $\widetilde{\kappa}_{tr}$ which are of order $10^{-4}-10^{-11}$, and sensitivities to $\widetilde{\kappa}_{0+}$ of

order 10⁻¹⁵. In some instances the sensitivity is several orders of magnitude worse than the best present limits for the other photon parameters (see above), and therefore, we will set all other photon parameters to zero. In other instances we just set the 10 polarization dependent components to zero as they have been measured to parts in 10³². In all cases these substitutions simplify the resulting expressions without affecting our conclusions.

II. LIMITS ON $\tilde{\kappa}_{_{tr}}$ FROM PREVIOUS EXPERIMENTS

Classical tests of special relativity (or Lorentz invariance) are usually grouped into three classes: Michelson-Morley (MM)¹⁹, Kennedy-Thorndike (KT)²⁰ and Ives-Stilwell (IS) experiments²¹. The later is sometimes referred to as Doppler, clock-comparison or one-way speed of light experiments. As mentioned above, MM and KT experiments have already been used to set stringent limits on a number of SME parameters in the photon sector. In this section we analyse IS experiments in the SME and derive the limit on $\tilde{\kappa}_{tr}$ obtained from the most sensitive such experiments to date ²².

In the original IS experiment 21 hydrogen atoms were moving at $v_{av}/c \approx 0.005$ (c = 299 792 458 m/s) with respect to the lab and the Doppler shifted frequencies of the H_{β} line in parallel (v_p) and anti-parallel (v_a) directions with respect to v_{at} are measured and compared (see fig. 1). The results are then used to determine whether the combination $v_p v_a/v_0^2 = 1$ as required in special relativity (where v_0 is the frequency for $v_{at}=0$).

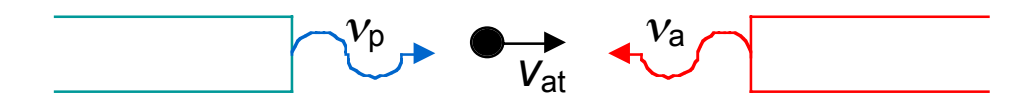


Figure 1: Principle of the Ives-Stilwell experiment. The Doppler shifted resonant frequencies of a moving atom are measured in the parallel v_p , and anti-parallel v_a directions.

Modern experiments of this type include Mössbauer rotor experiments²³, two photon and saturation spectroscopy experiments on atoms or ions ^{22, 24, 25}, or experiments that compare atomic clocks over large distances ²⁶⁻²⁸. Broadly speaking, all such experiments search for an anisotropy of the first order Doppler shift (or the one-way phase velocity of light) although some caution is required when physically interpreting such statements (in particular one needs to unambiguously define the meaning of "one-way light velocity"). More rigorously, all such experiments have been interpreted in the theoretical framework of Robertson, Mansouri and Sexl (RMS) ^{5, 6} in which they set limits on the parameter α_{MS} (one of the three fundamental RMS parameters, the other two being determined by MM and KT experiments). Limits on α_{MS} are obtained from ^{25 27} that limit $|\alpha_{MS} + 1/2| \le 8 \times 10^{-7}$ and, very recently, by ²² which provides the best limit to date $|\alpha_{MS} + 1/2| \le 2.2 \times 10^{-7}$.

As shown in ^{9, 11} (see also Sect. II. below) the modified Maxwell equations (1), (2) of the SME lead to effects on light propagation, in particular, a dependence of the phase velocity of the light on polarization and direction of propagation. This suggests that IS

experiments are sensitive to the SME. It turns out that they are in fact sensitive to the atpresent undetermined parameter $\tilde{\kappa}_{tr}$ via the difference of the phase velocities of signals travelling in opposite directions in a lab frame moving with respect to the sun centred frame. Meanwhile, MM and KT experiments always measure or compare return travel times of light signals, hence the phase velocity difference between the opposing directions cancels in the observables of those experiments, which makes them insensitive to $\tilde{\kappa}_{tr}$. In the next subsections we explicitly derive the sensitivity to $\tilde{\kappa}_{tr}$ for the most accurate IS experiment to date 22 .

A. Vacuum light propagation in the SME

Here we consider solutions to equations (1) and (2) in vacuum i.e. with the tensors $\ddot{\varepsilon}_r$ and $\ddot{\mu}_r$ in (2) being identity matrices. The more general case of magnetic and/or dielectric materials in the SME is treated in section III. Detailed calculations deriving the plane wave solutions in vacuum in the SME can be found in ^{9, 11}. Here we recall only the principles and results of those calculations that are relevant to our purpose.

We start with the standard ansatz

$$\mathbf{E} = \mathbf{E}_0 e^{i(\beta z - \omega t)}$$

$$\mathbf{B} = \mathbf{B}_0 e^{i(\beta z - \omega t)}$$
(4)

for a plane wave propagating in the positive z direction with frequency ω and wave number β . Substituting (4) into (1c), solving for **B**. Then substituting the result into (2) and (1d) results in a set of three linear coupled equations that can be solved for $E^{9, 11}$. A non-trivial solution is found only under the condition

$$\beta_{\pm} = \frac{1}{\sqrt{\varepsilon_0 \mu_0}} (1 - \rho \mp \sigma) |\omega| \tag{5}$$

where the \pm signs refer to two fundamental modes of propagation E_{\pm} with

$$\rho = -\frac{1}{4} \left(\kappa_{DE}^{xx} - \kappa_{HB}^{xx} + \kappa_{DE}^{yy} - \kappa_{HB}^{yy} + 2\kappa_{DB}^{xy} + 2\kappa_{HE}^{xy} \right)
\sigma^{2} = \left(\frac{1}{4} \left(\kappa_{DB}^{xx} - \kappa_{HE}^{xx} \right) - \frac{1}{4} \left(\kappa_{DB}^{yy} - \kappa_{HE}^{yy} \right) - \frac{1}{2} \left(\kappa_{DE}^{xy} + \kappa_{HB}^{xy} \right) \right)^{2}
+ \left(-\frac{1}{4} \left(\kappa_{DE}^{xx} + \kappa_{HB}^{xx} \right) + \frac{1}{4} \left(\kappa_{DE}^{yy} + \kappa_{HB}^{yy} \right) - \frac{1}{2} \left(\kappa_{DB}^{xy} - \kappa_{HE}^{xy} \right) \right)^{2}$$
(6)

to first order in κ . The dispersion relation (5) characterizes the propagation of two fundamental modes with the general solution for arbitrary polarization being a superposition of those two modes. By finding the explicit solutions for the two modes ⁹, it can be shown that, to first order in κ , the fields \mathbf{E}_{\pm} are perpendicular to each other and also perpendicular to the direction of propagation. In the absence of Lorentz violation

all κ components vanish, $\rho = \sigma = 0$, and (5) reduces to the usual dispersion relation in vacuum.

B. The Ives-Stilwell experiment in the SME

The most recent version 22 of the IS experiment is in principle very similar to the original experiment (c.f. Fig. 1). It uses collinear saturation spectroscopy on $^7\text{Li}^+$ ions moving at $v_{at}/c = 0.064$ in the heavy-ion storage ring TSR in Heidelberg. A closed two level transition at $v_0 = 5.46 \times 10^{14}$ Hz is excited by two iodine stabilised lasers which are tuned to the Doppler shifted transition frequencies (v_p and v_a). The observed fluorescence signal of the ions shows a Lamb dip characteristic of saturation spectroscopy when both lasers are resonant with the respective Doppler shifted frequencies. Combining the two frequencies the experiment then determines

$$\frac{v_p v_a}{v_0^2} = 1 + \varepsilon_{LV}(t) \tag{7}$$

where ε_{LV} is a term, in general time varying, that characterises possible Lorentz violation in a given theoretical framework. In special relativity $\varepsilon_{LV} = 0$, and the experiment by Saathoff et al. 22 sets a limit of $\varepsilon_{LV} < 1.8 \times 10^{-9}$. They interpret their result in the theoretical framework of Robertson, Mansouri and Sexl 5,6 (RMS) in which $\varepsilon_{LV} = 2(\alpha_{RMS} + 1/2)(\mathbf{v}_{at}^2 + 2\,\mathbf{v}_{lab}\cdot\mathbf{v}_{at})/c^2$ where \mathbf{v}_{lab} is the velocity of the laboratory in the preferred frame (generally taken as the rest frame of the cosmic microwave background). They obtain a limit of $(\alpha_{RMS} + 1/2) < 2.2 \times 10^{-7}$ under the assumption that $\mathbf{v}_{at} >> \mathbf{v}_{lab}$.

To interpret the experiment in the SME we first work in an "experiment" frame which is at rest in the laboratory with the atoms moving along its positive z-axis (see fig. 1). In that frame the two laser frequencies are v_p and v_a respectively. Using (5) we define the phase velocities of the parallel and anti-parallel laser beams

$$c_{p} = \frac{\omega_{p}}{\beta_{p}} = c(1 + \rho_{p} \pm \sigma_{p})$$

$$c_{a} = \frac{\omega_{a}}{\beta_{a}} = c(1 + \rho_{a} \pm \sigma_{a})$$
(8)

with ρ_p and σ_p given by (6) and ρ_a and σ_a obtained from (6) by changing the sign of all κ_{DB} and κ_{HE} terms. The \pm sign again refers to the two fundamental modes, and all quantities (in particular the κ tensors) are defined in the "experiment" frame.

We then calculate the time interval (in the experiment frame) between two successive maxima of the parallel and anti-parallel beams encountered by an atom. These are equal to the Doppler shifted periods in the experiment frame $(1/v_p)$ and $1/v_a$) of the light encountered by the atom:

$$v'_{p} = v_{p}(1 - v_{at}/c_{p}) v'_{a} = v_{a}(1 + v_{at}/c_{a})$$
(9)

where v_{at} is the atomic velocity in the experiment frame.

To obtain the frequencies (v_p) and v_a and v_a as seen by the atom (the frequencies absorbed by the atom) we need to transform to the "atom" frame, co-moving with the atom. Using a standard Lorentz transformation (justified below) and imposing that the light absorbed by the atom be resonant with the chosen transition (i.e. setting v_p " = v_a " = v_0) we obtain

$$v_p = v_0 \frac{\sqrt{1 - v_{at}^2 / c^2}}{1 - v_{at} / c_p}$$
 and $v_a = v_0 \frac{\sqrt{1 - v_{at}^2 / c^2}}{1 + v_{at} / c_a}$ (10)

which relates the rest frequency v_0 of the atomic transition to the measured frequencies of the two lasers on resonance (v_p and v_a).

To obtain expression (10) we have used a standard Lorentz transformation to transform the atomic transition frequency from the atom to the experiment frame. That is because we assume throughout this work that the matter sector (and therefore the atomic transition frequency) is Lorentz invariant. Even if this was not the case, any Lorentz violation in the atomic transition frequency would only affect that last transformation, i.e. the v_{at}^2/c^2 terms in (10), which are of second order with respect to the leading order Lorentz violating terms in $v_{at}/c_{p/a}$.

Combining the two equations of (10) and keeping only first order terms in v_{at}/c we finally obtain an expression for the observable in 22

$$\frac{v_a v_p}{v_0^2} = 1 + \frac{v_{at}}{c_p} - \frac{v_{at}}{c_a} \tag{11}$$

where the Lorentz violating terms are contained in the phase velocities c_a and c_p defined in (8), and expressed using (6) in the experiment frame (with all κ tensors defined in the experiment frame).

We then transform the κ tensors to a laboratory frame as defined in 11 (x-axis pointing south, z-axis vertically upwards) by a simple rotation, and to the conventional sun-centred frame by a rotation and a boost (equations (30) and (31) of 11). As mentioned above, the sensitivities to κ_{tr} discussed here are orders of magnitude worse than the best present limits on all other κ components. We therefore set those to zero in our final expression in the sun-centred frame, which leaves, after some calculation,

$$\frac{v_{a}v_{p}}{v_{0}^{2}} = 1 + 4\widetilde{\kappa}_{tr} \frac{v_{at}}{c} \begin{bmatrix}
\cos(\phi) \frac{v_{\oplus}}{c} \left(\cos(\Omega_{\oplus}T)(\sin(\eta)\sin(\chi) - \cos(\eta)\cos(\chi)\sin(\omega_{\oplus}T_{\oplus})) + \sin(\Omega_{\oplus}T)\cos(\chi)\cos(\omega_{\oplus}T_{\oplus}) \\
+ \sin(\phi) \left(\frac{v_{r}}{c} - \frac{v_{\oplus}}{c}(\cos(\Omega_{\oplus}T)\cos(\eta)\cos(\omega_{\oplus}T_{\oplus}) + \sin(\Omega_{\oplus}T)\sin(\omega_{\oplus}T_{\oplus}))\right)
\end{bmatrix}$$
(12)

For the derivation of (12) we have assumed that the atoms move horizontally with a velocity v_{at} in the lab frame and at an angle ϕ with respect to local south. The other symbols follow the definitions in ¹¹: η is the declination of the Earth's orbital plane ($\eta \approx 23.4^{\circ}$), χ is the colatitude of the laboratory, Ω_{\oplus} , v_{\oplus} are the angular velocity and speed of the Earth's orbital motion, ω_{\oplus} is the angular velocity of the Earth's rotation, and $v_r = r_{\oplus}\omega_{\oplus}\sin(\chi)$ is the velocity of the lab due to rotation of the Earth. The times T and T_{\oplus} are the time since a spring equinox and the time since the lab frame y-axis pointed towards 90 ° right ascension respectively.

The experiment by Saathoff et al. 22 sets an upper limit of 1.8×10^{-9} on the deviation of $v_p v_a / v_0^2$ from unity. Using (12) that result implies a limit on $\tilde{\kappa}_{tr}$ of the order 10^{-4} , with the exact value depending on the angle ϕ and the times (T and T_{\oplus}) at which the experiment was carried out. This is, to our knowledge, the only quoted limit on $\tilde{\kappa}_{tr}$ to date. However, the cavity experiments that are directly sensitive to the even parity coefficients are also expected to be sensitive to second order in velocity on $\tilde{\kappa}_{tr}^{40}$. Since the value of the earth's orbital velocity is of order 10^{-4} (with respect to c), and the best cavity experiments have a sensitivity of order 10^{-15} to the even parity coefficients, a sensitivity of 10^{-7} is expected. Detailed second order perturbation analysis would be necessary to calculate and verify the exact sensitivity. To improve on this sensitivity, a null experiment is proposed in section III.

III. INTERFEROMETER TESTS USING MAGNETIC MATERIALS

In the previous section we have shown that the $\tilde{\kappa}_{tr}$ scalar may be measured by Ives-Stilwell experiments, and set a constraint on its value of parts in 10^4 . In general, experiments that are sensitive to the $\tilde{\kappa}_{tr}$ scalar, but suppressed by the boost, are also directly sensitive to the odd parity coefficient of the $\tilde{\kappa}_{0+}$ tensor (see appendix A, and a recent submission that proposes a static electromagnetic test 29). Cavity resonator experiments have only constrained these parameters to parts in 10^{11} indirectly through the boost dependence $^{14, 15}$. In contrast, the same experiments have measured the parity even parameters directly at parts in 10^{15} . The boost dependence suppresses the sensitivity by the ratio of the earth's orbital speed to the speed of light, which is of order 10^{-4} .

In this section we consider the possibility of testing the 'one-way' properties of electromagnetic radiation using a Mach-Zehnder (MZ) interferometer, with a much higher sensitivity than the Ives-Stilwell experiments. Interferometers offer the possibility of very sensitive tests at microwave $^{30, 31}$ and optical frequencies 32 . For this concept to work, each arm of the interferometer must have a different phase dependence on $(\kappa_{DB})_{lab}$. In this section we show that this is possible if one arm of the interferometer is filled with a magnetic medium. Also, we introduce a recycling technique based on a travelling wave resonator, and show that a sensitivity of order 10^{-15} is possible.

The description of electrodynamics in the photon sector of the SME is essentially an extension of Maxwell's equations, where similar SME equations can be written as shown in equation (1). However, the Lagrangian of the SME in the photon sector necessitates that the constitutive relations, given by equation (2), are more general. For the purpose of this work it is sufficient if we assume that the permeability and permittivity are isotropic. This means that the $\ddot{\varepsilon}_r$ and $\ddot{\mu}_r$ tensors are diagonal with all three components equal to the scalar permittivity and permeability given by ε_r and μ_r respectively. It is implicit in the form of the SME equation (2) that the matter sector does not contribute to the Lorentz violating parameters, as they are not altered in any way by the magnetization or polarization of the material.

A. Plane wave solution in an isotropic medium

Using the SME equations given in (1) and (2), the simple problem of uniform plane wave propagation in an infinite isotropic medium is considered. Since an interferometer measures phase, the idea here is to calculate the effects of the odd parity and scalar Lorentz violating terms on the propagation constant of the plane wave. Lorentz violating effects are expected to be small and only differ slightly from the solution to Maxwell's equations. For the purposes of this work we assume $\sigma = 0$ in (5). This is equivalent to setting 10 of the 19 possible Lorentz violating parameters to zero, which have been measured very accurately in astrophysical tests at parts in 10^{32} ¹². This means it is not necessary to decompose the solution into the two birefringent components as the solution is independent of polarization. From this assumption we proceed to calculate the effect of the remaining Lorentz violating terms on the propagation of plane and guided waves in isotropic media.

First, in the laboratory frame it is assumed that the plane wave is propagating in the z direction at a frequency ω and propagation constant β , and thus the electric and magnetic fields have the form;

$$\boldsymbol{E} = \left(E_{xo}\hat{\boldsymbol{x}} + E_{yo}\hat{\boldsymbol{y}} + E_{zo}\hat{\boldsymbol{z}}\right)e^{-i\beta z}e^{i\omega t}$$
(13)

$$\boldsymbol{H} = (H_{xo}\hat{\boldsymbol{x}} + H_{vo}\hat{\boldsymbol{y}} + H_{zo}\hat{\boldsymbol{z}})e^{-i\beta z}e^{i\omega t}$$
(14)

Then, by substituting (13) and (14) into (2) the flux densities D and B may be calculated in terms of the amplitudes of E and H. Then by substituting E and B into (1c) and H and D into (1d), to leading order in the Lorentz violating terms, one can show that $E_{zo} \sim H_{zo} \sim 0$ and one is left to solve the following leading-order equation;

$$\begin{bmatrix} -\varepsilon_{r} - (\kappa_{DE})_{lab}^{xx} & 0 & 0 & \xi - \mu_{r}(\kappa_{DB})_{lab}^{xy} \\ 0 & -\varepsilon_{r} - (\kappa_{DE})_{lab}^{yy} & -\xi - \mu_{r}(\kappa_{DB})_{lab}^{yx} & 0 \\ 0 & \xi - \mu_{r}(\kappa_{HE})_{lab}^{xy} & \mu_{r} - \mu_{r}^{2}(\kappa_{HB})_{lab}^{yy} & 0 \\ -\xi - \mu_{r}(\kappa_{HE})_{lab}^{yx} & 0 & 0 & \mu_{r} - \mu_{r}^{2}(\kappa_{HB})_{lab}^{yy} \end{bmatrix} \begin{bmatrix} E_{xo} \\ E_{yo} \\ \sqrt{\frac{\mu_{o}}{\varepsilon_{o}}} H_{xo} \\ \sqrt{\frac{\varepsilon_{o}}{\varepsilon_{o}}} H_{yo} \end{bmatrix} = 0$$
(15)

Here all κ matrices are written in the laboratory frame and $\xi = \beta c/\omega$ or β/k_0 , where $k_0 = 2\pi/\lambda_v$, is the propagation constant as calculated in vacuum with no Lorentz violating terms and λ_v , is the wavelength in vacuum.

Non-trivial solutions are obtained when the determinant of the 4 by 4 matrix of (15) is set to zero. There are four solutions relating to two polarizations travelling positively and negatively along the z direction. To leading order in the κ matrix components, the propagation constants are calculated to be;

$$\frac{\beta_{xy}^{+}}{k} = 1 + \sqrt{\frac{\mu_r}{\varepsilon_r} (\kappa_{DB})_{lab}^{xy}} + \frac{1}{2\varepsilon_r} (\kappa_{DE})_{lab}^{xx} - \frac{\mu_r}{2} (\kappa_{HB})_{lab}^{yy}$$
(16a)

$$\frac{\beta_{xy}^{-}}{k} = -1 + \sqrt{\frac{\mu_r}{\varepsilon_r}} (\kappa_{DB})_{lab}^{xy} - \frac{1}{2\varepsilon_r} (\kappa_{DE})_{lab}^{xx} + \frac{\mu_r}{2} (\kappa_{HB})_{lab}^{yy}$$
(16b)

$$\frac{\beta_{yx}^{+}}{k} = 1 - \sqrt{\frac{\mu_r}{\varepsilon_r}} (\kappa_{DB})_{lab}^{yx} + \frac{1}{2\varepsilon_r} (\kappa_{DE})_{lab}^{yy} - \frac{\mu_r}{2} (\kappa_{HB})_{lab}^{xx}$$
(16c)

$$\frac{\beta_{yx}^{-}}{k} = -1 - \sqrt{\frac{\mu_r}{\varepsilon_r}} (\kappa_{DB})_{lab}^{yx} - \frac{1}{2\varepsilon_r} (\kappa_{DE})_{lab}^{yy} + \frac{\mu_r}{2} (\kappa_{HB})_{lab}^{xx}$$
 (16d)

The superscript refers to the sign of the direction of propagation along the z-axis, the subscripts label the directions of the E and H field polarisations respectively, and $k = \sqrt{\varepsilon_r \mu_r} . k_o$ is the propagation constant of the plane wave in the medium. If the κ matrices are set to zero we retrieve the well-known solutions to Maxwell's equations. For the Maxwell solution there is no dependence of polarization on the propagation constant in an isotropic media. This is also true for the SME calculation of (16), as we have set $\sigma = 0$ and the final sensitivity to the coefficients of the $\tilde{\kappa}_{0+}$ tensor and the $\tilde{\kappa}_{tr}$ scalar are independent of polarization. It is also interesting to note that the coefficients of the $(\kappa_{DB})^{jk}_{lab}$ terms are the square root of the relative permeability divided by the relative permittivity. It is these coefficients that makes the experiment sensitive to the odd parity and scalar coefficients when we transform to the sun centred celestial frame from the laboratory frame (see appendix A). Low loss media at microwave frequencies have permittivity greater than 1 and permeability equal to or less than 1, thus all coefficient in (16) must be less than 1 if a sensitive measurement is to be made.

Now from (16) we can make a general calculation of the phase shift recorded by a MZ interferometer with two arms containing two different media as shown in figure 2, and with plane waves travelling in the positive z direction.

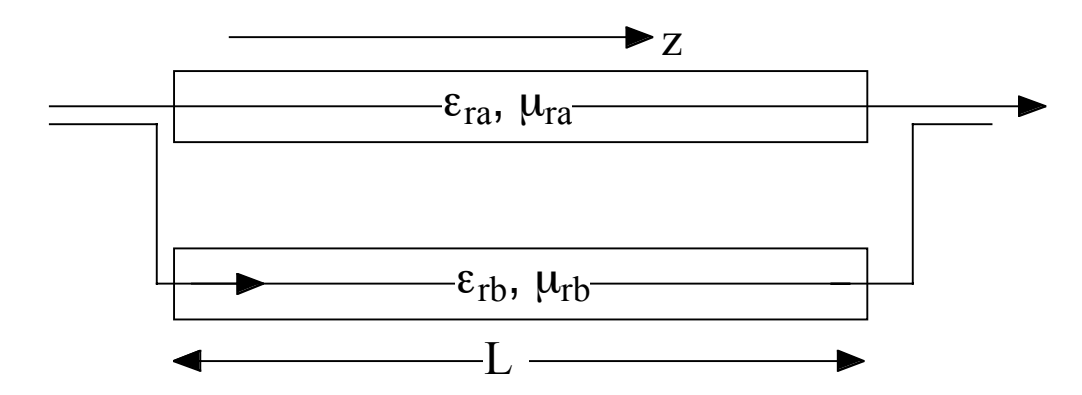


Figure 2. Mach-Zehnder (MZ) interferometer of length L, with two arms of permittivity ε_{ra} and ε_{rb} , and permeability of μ_{ra} and μ_{rb} respectively.

For the above MZ interferometer of length L, the phase shift at the output is given by the difference of phase gained along the arms a and b. For the (y, x) and (x, y) polarisations it is given by;

$$\Delta \theta_{xy}^{+} = \theta_{xya}^{+} - \theta_{xyb}^{+} = \frac{2\pi L}{\lambda_{v}} \left[\frac{\left(\sqrt{\mu_{ra}\varepsilon_{ra}} - \sqrt{\mu_{rb}\varepsilon_{rb}}\right) + \left(\mu_{ra} - \mu_{rb}\right)\kappa_{DBlab}^{xy} + \frac{1}{2} \left(\sqrt{\frac{\mu_{ra}}{\varepsilon_{ra}}} - \sqrt{\frac{\mu_{rb}}{\varepsilon_{rb}}}\right)\kappa_{DElab}^{xx} - \frac{1}{2} \left(\sqrt{\mu_{ra}^{3}\varepsilon_{ra}} - \sqrt{\mu_{rb}^{3}\varepsilon_{rb}}\right)\kappa_{HBlab}^{yy} \right]$$

$$(17)$$

$$\Delta\theta_{yx}^{+} = \theta_{yxa}^{+} - \theta_{yxb}^{+} = \frac{2\pi L}{\lambda_{v}} \left[\left(\sqrt{\mu_{ra} \varepsilon_{ra}} - \sqrt{\mu_{rb} \varepsilon_{rb}} \right) - \left(\mu_{ra} - \mu_{rb} \right) \kappa_{DBlab}^{yx} + \frac{1}{2} \left(\sqrt{\frac{\mu_{ra}}{\varepsilon_{ra}}} - \sqrt{\frac{\mu_{rb}}{\varepsilon_{rb}}} \right) \kappa_{DElab}^{yy} - \frac{1}{2} \left(\sqrt{\mu_{ra}^{3} \varepsilon_{ra}} - \sqrt{\mu_{rb}^{3} \varepsilon_{rb}} \right) \kappa_{HBlab}^{xx} \right]$$

$$(18)$$

In general there is a constant phase difference between the two arms, and a modified sensitivity to the Lorentz violating coefficients depending on the permittivity and permeability of each arm. From (17) and (18) it is evident that the coefficients of the $(\kappa_{DB})^{xy}_{lab}$ and $(\kappa_{DB})^{yx}_{lab}$ terms only depends on the magnetic properties of the two arms and not the dielectric. The reason is because of two competing effects. First, the sensitivity is reduced by the square root of the permittivity due to the nature of the SME solution from (1) and (2). This is compensated by an increase in phase sensitivity due to the phase length of the interferometer arm being enhanced by the same amount, so the phase shift becomes independent of permittivity. Conversely, for the permeability the two effects

enhance the signal rather than cancel, so the phase shift becomes proportional to permeability.

The sensitivity of this experiment is proportional to the interferometer arm length divided by the wavelength, which is equal to the number of wavelengths along the arm of the interferometer. Thus, the sensitivity may be increased with long arms and short wavelengths. A further method to improve the sensitivity is through resonant recycling techniques, which have been developed at both microwave and optical frequencies. These techniques typically improve phase sensitive measurements by two orders of magnitude $^{30-32}$. For this configuration we assume different values of permeability in each arm of the interferometer as shown in figure 3. For this analysis we will only consider the (y, x) polarization in (18), (16c) and (16d), as the solution is independent of which one we choose. Also, we only keep the desired response to the $(\kappa_{DB})^{yx}_{lab}$ coefficient, with N and M the number of recycles in each arm.

$$\Delta\theta_{yx} = \left((N+1)\theta_{yx,a}^{+} + N\theta_{yx,b}^{-}\right) - \left((M+1)\theta_{yx,b}^{+} + M\theta_{yx,b}^{-}\right)$$

$$= -(N+1)\frac{2\pi L}{\lambda_{v}}\left[\left(\mu_{ra} - \mu_{rb}\right)\left(\kappa_{DB}\right)_{lab}^{yx}\right]$$

$$\mu_{rb}$$

$$\mu_{rb}$$

$$\mu_{rb}$$

$$\mu_{rb}$$

$$\mu_{rb}$$

$$\mu_{rb}$$

Figure 3. Resonant-recycling technique to enhance the sensitivity to the measurement of $(\kappa_{DB})_{lab}^{yx}$.

The phase shift turns out to be independent of the number of M recycles but proportional to N. This is because the arm with N recycles has the parity broken by the dissimilar forward and return paths, which permits an enhancement in sensitivity directly to the parity-odd coefficients. Conversely, the other arm does not, however, M is required to be non-zero so the dispersion in both arms will be similar, and the phase noise of the oscillator driving the interferometer will be suppressed. The parity-odd resonant recycling arm is essentially an asymmetric travelling wave resonator. The same principle may be used to make the frequency of a resonant cavity directly sensitive to the odd parity coefficients.

B. Perturbation equation for waveguides in the SME

It is more practical to use transmission lines and waveguides to propagate waves in an interferometer at microwave frequencies, while at optical frequencies the plane wave solution may be kept, unless optical fibers are used as a means of transmission. In this section we derive a technique to calculate the effects of the guiding medium in the SME as long as $\sigma = 0$ in (5). The difficulties encountered in solving boundary-valued problems in the SME are greater than with Maxwell's equations or for the leading-order plane wave SME solution given in (16a-d). In this section we aim for a more general solution that implements perturbation analysis so the leading order solution may be calculated from fields derived from Maxwell's equations. This analysis is similar to that of Kostelecky and Mewes, which calculates the leading order perturbation in frequency for a resonant cavity ¹¹. The analysis starts with the quadratic lemma for two electromagnetic processes (E_0 , H_0 , D_0 , B_0) and (E, H, D, B) at different oscillation frequencies, ω_0 and ω ;

$$\nabla \cdot (\mathbf{E} \times \mathbf{H}_{0}^{*} + \mathbf{E}_{0}^{*} \times \mathbf{H}) + i\omega \mathbf{H}_{0}^{*} \cdot \mathbf{B} - i\omega_{0} \mathbf{B}_{0}^{*} \cdot \mathbf{H} + i\omega \mathbf{E}_{0}^{*} \cdot \mathbf{D} - i\omega_{0} \mathbf{D}_{0}^{*} \cdot \mathbf{E} = 0$$
 (20)

We base our analysis on the perturbation method, which has been used by Gurevich³³ for computing perturbed propagation constants of modes in waveguides due to a small perturbing object. In this case we use a similar technique, but regard the SME fields as perturbations of the Maxwell fields. Here we assume that the fields (E_0, H_0, D_0, B_0) are the Maxwell fields given by (2) when the κ matrices are set to zero, and that (E, H, D, B) are the SME fields given by (2) when the κ matrices are non-zero. Thus, by substituting (2) into (20) we can derive the fundamental Lemma of the SME in the photon sector;

$$\nabla \cdot (\boldsymbol{E} \times \boldsymbol{H}_{0}^{*} + \boldsymbol{E}_{0}^{*} \times \boldsymbol{H}) = i \frac{\omega_{0}}{\mu_{0}} \boldsymbol{B}_{0}^{*} \cdot \ddot{\boldsymbol{\mu}}_{r}^{-1} \cdot \boldsymbol{B} - i \frac{\omega}{\mu_{0}} \ddot{\boldsymbol{\mu}}_{r}^{-1*} \cdot \boldsymbol{B}_{0}^{*} \cdot \boldsymbol{B} + i \omega_{0} \varepsilon_{0} \ddot{\boldsymbol{\varepsilon}}_{r}^{*} \cdot \boldsymbol{E}_{0}^{*} \cdot \boldsymbol{E} - i \omega \varepsilon_{0} \boldsymbol{E}_{0}^{*} \cdot \ddot{\boldsymbol{\varepsilon}}_{r} \cdot \boldsymbol{E} + i \omega_{0} \varepsilon_{0} \ddot{\boldsymbol{\varepsilon}}_{r}^{*} \cdot \boldsymbol{E}_{0} \cdot \boldsymbol{E} - i \omega \varepsilon_{0} \boldsymbol{E}_{0}^{*} \cdot \ddot{\boldsymbol{\varepsilon}}_{r} \cdot \boldsymbol{E} + i \omega_{0} \varepsilon_{0} \ddot{\boldsymbol{\varepsilon}}_{r}^{*} \cdot \boldsymbol{E} + i \omega_{0} \ddot{\boldsymbol{\varepsilon}}_{0} \dot{\boldsymbol{\varepsilon}}_{r}^{*} \cdot \boldsymbol{E} + i \omega_{0} \ddot{\boldsymbol{\varepsilon}}_{0} \ddot{\boldsymbol{\varepsilon}}_{r}^{*} \cdot \boldsymbol{E} + i \omega_{0} \ddot{\boldsymbol{\varepsilon}}_{0} \ddot{\boldsymbol{\varepsilon}}_{0$$

This Lemma may be used to calculate the frequency perturbation in the SME of a resonator ¹¹. For our case we use the Lemma to calculate the perturbation of the propagation constant for a guided wave. Here, we assume the frequency in the SME is the same for a propagating mode as calculated by Maxwell's equations, so that $\omega = \omega_0$. Also, we apply the relationship $\kappa_{DB} = -\kappa_{HE}^T$, to further simplify the analysis. Finally, if the permittivity and permeability tensors are Hermitian (as is the case for isotropic to gyrotropic media) then the first four terms on the right-hand side of equation (21) cancel, and it becomes;

$$\nabla \cdot (\boldsymbol{E} \times \boldsymbol{H}_{0}^{*} + \boldsymbol{E}_{0}^{*} \times \boldsymbol{H}) = i\omega_{0} \left(-\varepsilon_{0} \boldsymbol{E}_{0}^{*} \cdot \kappa_{DE} \cdot \boldsymbol{E} + \frac{1}{\mu_{0}} \boldsymbol{B}_{0}^{*} \cdot \kappa_{HB} \cdot \boldsymbol{B} - 2\sqrt{\frac{\varepsilon_{0}}{\mu_{0}}} \boldsymbol{E}_{0}^{*} \cdot \kappa_{DB} \cdot \boldsymbol{B} \right)$$
(22)

The solutions will be travelling waves so we may assume they are of the form;

$$E = E_c e^{-i\beta z}, H = H_c e^{-i\beta z}, E_0 = E_{0c} e^{-i\beta_0 z}, H_0 = H_{0c} e^{-i\beta_0 z}$$
 (23)

Here β_0 is the propagation constant calculated by Maxwell's equations and β is the propagation constant in the SME. Substituting (23) into (22) and integrating over the surface shown in figure 4 (22) becomes;

$$\int_{L} (\boldsymbol{E}_{c} \times \boldsymbol{H}_{0c}^{*} + \boldsymbol{E}_{0c}^{*} \times \boldsymbol{H}_{c}) . \boldsymbol{n}_{0} dL - i (\beta - \beta_{0}) \int_{S} (\boldsymbol{E}_{c\perp} \times \boldsymbol{H}_{0c\perp}^{*} + \boldsymbol{E}_{0c\perp}^{*} \times \boldsymbol{H}_{c\perp}) . \boldsymbol{z}_{0} dS$$

$$= i \omega_{0} \int_{S} \left(-\varepsilon_{0} \boldsymbol{E}_{0c}^{*} . \kappa_{DE} . \boldsymbol{E}_{c} + \frac{1}{\mu_{0}} \boldsymbol{B}_{0c}^{*} . \kappa_{HB} . \boldsymbol{B}_{c} - 2 \sqrt{\frac{\varepsilon_{0}}{\mu_{0}}} \boldsymbol{E}_{0c}^{*} . \kappa_{DB} . \boldsymbol{B}_{c} \right) dS \tag{24}$$

Here n_0 is a unit vector along the normal to the curve \mathcal{L} , which lies in the plane of the waveguide cross section, z_0 is a unit vector along the waveguide axis and the \perp subscript defines the part of the E and H field vectors perpendicular to the propagation (ie. not including the z components).

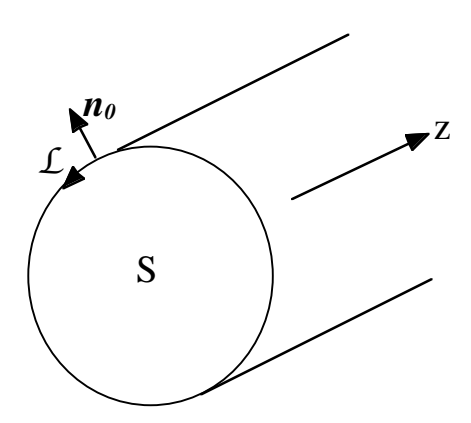


Figure 4. Cross-section of the transmission medium

Assuming no Lorentz violation in the matter sector, the boundary conditions of the tangential electric field in the photon sector of the SME, have been shown to be equal to zero, equivalent to the Maxwell case ¹¹. Thus, the first term in (24) is zero. Thus, to calculate the leading order effects on the propagation constant we replace the perturbed SME fields with the unperturbed Maxwell fields and equate imaginary parts on both sides of equation (24), to give;

$$\beta - \beta_0 = ck_0 \frac{\int_{S}^{I} \left(\varepsilon_0 \boldsymbol{E}_{0a}^* . \kappa_{DE} . \boldsymbol{E}_{0a} - \frac{1}{\mu_0} \boldsymbol{B}_{0a}^* . \kappa_{HB} . \boldsymbol{B}_{0a} + 2 \operatorname{Re} \left[\sqrt{\frac{\varepsilon_0}{\mu_0}} \boldsymbol{E}_{0a}^* . \kappa_{DB} . \boldsymbol{B}_{0a} \right] \right) dS}{\int_{S} \left(\boldsymbol{E}_{0a\perp} \times \boldsymbol{H}_{0a\perp}^* + \boldsymbol{E}_{0a\perp}^* \times \boldsymbol{H}_{0a\perp} \right) . z_0 dS}$$
(25)

However, the observable for an interferometer experiment is the phase difference between the two arms $\Delta\theta$. Thus, in the laboratory frame we may rewrite (25) in terms of phase shift for a single mode propagating along a single waveguide as;

$$\theta = (\beta - \beta_0)L = (\mathcal{M}_{DE})_{lab}^{jk} (\kappa_{DE})_{lab}^{jk} + (\mathcal{M}_{HB})_{lab}^{jk} (\kappa_{HB})_{lab}^{jk} + (\mathcal{M}_{DB})_{lab}^{jk} (\kappa_{DB})_{lab}^{jk}$$
(26)

where L is the length of propagation along the z-axis and,

$$\left(\mathcal{M}_{DE}\right)_{lab}^{jk} = \frac{2\pi L}{\lambda_{v}} \frac{\int_{S} \left(\sqrt{\frac{\varepsilon_{0}}{\mu_{0}}} \boldsymbol{E}_{0a\perp}^{j*} \cdot \boldsymbol{E}_{0a}^{k}\right) dS}{\int_{S} \left(\boldsymbol{E}_{0a\perp} \times \boldsymbol{H}_{0a\perp}^{*} + \boldsymbol{E}_{0a\perp}^{*} \times \boldsymbol{H}_{0a\perp}\right) \cdot \boldsymbol{z}_{0} dS}$$
(27a)

$$\left(\mathcal{M}_{HB}\right)_{lab}^{jk} = \frac{2\pi L}{\lambda_{v}} \frac{-\int_{S} \left(\frac{1}{\sqrt{\varepsilon_{0}\mu_{0}^{3}}} B_{0a}^{j*} B_{0a}^{k}\right) dS}{\int_{S} \left(\boldsymbol{E}_{0a\perp} \times \boldsymbol{H}_{0a\perp}^{*} + \boldsymbol{E}_{0a\perp}^{*} \times \boldsymbol{H}_{0a\perp}\right) z_{0} dS}$$
(27b)

$$\left(\mathcal{M}_{DB}\right)_{lab}^{jk} = \frac{2\pi L}{\lambda_{v}} \frac{2\operatorname{Re}\left[\int_{S} \left(\frac{1}{\mu_{0}} \boldsymbol{E}_{0a}^{j*}.B_{0a}^{k}\right) dS\right]}{\int_{S} \left(\boldsymbol{E}_{0a\perp} \times \boldsymbol{H}_{0a\perp}^{*} + \boldsymbol{E}_{0a\perp}^{*} \times \boldsymbol{H}_{0a\perp}\right).z_{0} dS}$$
(27c)

Thus, if the Maxwell fields are known for the propagating solution, the phase shift due to a leading order Lorentz violating terms in the SME may be calculated. It is easily shown that equation (26) is consistent with the plane wave solution calculated previously.

For the general guided wave, the sensitivity to odd parity and scalar coefficients are proportional to the difference between the two coefficients $(\mathcal{M}_{DB})^{jk}_{lab} - (\mathcal{M}_{DB})^{kj}_{lab}$ ($j \neq k$), which is $\frac{2\pi L}{\lambda_v} \mu_r$ for the propagating plane wave. So far our calculations have shown this

value is independent of the guiding structure. For example, the calculation for TE modes in a rectangular waveguide is given in Appendix B. We have also undertaken this calculation for many different modes in many types of waveguides (but not presented here), including cylindrical, coaxial and helical guiding structures. In all cases the $(\mathcal{M}_{DB})_{lab}^{jk} - (\mathcal{M}_{DB})_{lab}^{kj}$ coefficient was the same as the plane wave case. For the interferometer experiment the observable is phase difference between two guided waves. The equivalent \mathcal{M} matrices for this case are then given by the difference of the two arms, which will be non-zero when the permeability is different.

In general the wave need not be propagating along the z direction of the laboratory frame. To calculate the \mathcal{M} tensors for a wave propagating along another arbitrary direction, the tensor must undergo a rotation. For the laboratory experiment it is practical to propagate along the y or x direction. In this case only a $\pi/2$ rotation is required. To detect the signal, we rely on the time dependence to modulate the phase, which can be determined in the standard way as described in Kostelecky and Mewes ¹¹ by transforming from the lab (rotating or non-rotating) to the sun centred celestial frame, as given in appendix A.

C. Proposed interferometer experiment

Sensitive interferometers have been developed at optical ³² and microwave frequencies 31, 34. However this experiment requires the availability of low loss magnetic material at the respective frequency. Low loss materials are only possible at microwave frequencies with relative permeability less than unity above the magnetic spin resonance of the material. For example, at microwave frequencies one could use YIG (Yttrium Iron Garnet), which has a permeability of about 0.9, and loss tangent of 10⁻⁴ at the frequency of 10 GHz 35 and in this paper we use this as our example experiment. Alternatively, at optical frequencies magnetic effects may be induced using magnetic polaritons ³⁶⁻³⁸, and if the ratio of length to wavelength can be increased a more sensitive measurement may be viable. The sensitivity of this type of experiment will be dependent on a host of other technical factors, like the available power from the frequency source, the phase balance between the interferometer arms etc. These dependencies have been largely discussed in the papers that implement low noise interferometers, and we leave out the details here. For our purposes we need to just quote the spectral density of the possible phase noise possible with current technology. Typically the best square root spectral density of phase noise $\sqrt{S_{\phi}}$, is of the order 10^{-10} rads/ $\sqrt{\text{Hz}}$, which is limited by thermal noise 31 . Chopping techniques to lock the interferometer output to a dark port (null measurement) can further reduce the flicker noise corner 32, and rotation of the experiment can ensure that the phase noise limit is reached. In this case the sensitivity of the phase measurement is dependent on the observation time and given by;

$$\delta\theta\big|_{SNR=1} = \frac{\sqrt{S_{\phi}}}{\sqrt{\tau_{obs}}} \tag{28}$$

If the *b* interferometer arms shown in figure 1 and 2 contain vacuum, then the signal due to the Lorentz violation given by (19) due to the $(\kappa_{DB})_{lab}^{jk}$ term is given by;

$$\Delta\theta = (N+1)\frac{2\pi L}{\lambda_{v}}(\mu_{ra} - 1)(\kappa_{DB})_{lab}^{jk}$$
(29)

This means the sensitivity of the $(\kappa_{DB})_{lab}^{jk}$ measurement may be given with a SNR of one (or significance of one standard deviation), when

$$\delta(\kappa_{DB})_{lab}^{jk}\Big|_{SNR=1} = \frac{\lambda_{\nu}}{2\pi L(N+1)(\mu_{r}-1)} \frac{\sqrt{S_{\phi}}}{\sqrt{\tau_{obs}}}$$
(30)

Thus for a 10 GHz interferometer of order one meter long with a recycling factor of N+1=50, the estimated sensitivity of $(\kappa_{DB})^{jk}_{lab}$ is of the order $10^{-13}/\sqrt{\tau_{obs}}$. Thus, a measurement over an hour will give a sensitivity of order 10^{-15} . This translates to sensitivity to κ_{tr} of order 10^{-11} and κ_{0+} of order 10^{-15} .

Acknowledgments

This work was supported by the Australian Research Council.

APPENDIX A: TRANSFORMATION OF PARITY-ODD AND SCALAR COEFFICIENTS TO THE SUN CENTRED CELESTIAL EQUATORIAL FRAME

In this appendix we undertake to calculate the time dependence of a general experiment sensitive to $\tilde{\kappa}_{tr}$ and $\tilde{\kappa}_{0+}$ coefficients with respect to the inertial sun centred celestial frame, in which the Lorentz violating coefficients are constant. To do this we set all terms with respect to the sun centred celestial frame to zero except for the $\tilde{\kappa}_{tr}$ and $\tilde{\kappa}_{0+}$ terms, as stringent limits by astrophysical and cavity experiments have already been set. This is attained by providing the action of rotations, R^{jJ} , and boosts, β^{J} , from the laboratory to the sun centred celestial frame in the same way as Kostelecky and Mewes, from the following transformations ¹¹.

$$\left(\kappa_{HB}\right)_{lab}^{jk} = T_0^{jkJK} \tilde{\kappa}_{HB}^{JK} - T_1^{kjKJ} \tilde{\kappa}_{DB}^{JK} - T_1^{jkKJ} \tilde{\kappa}_{DB}^{JK}$$
(A2)

$$\left(\kappa_{DB}\right)_{lab}^{Jk} = T_0^{jkJK} \tilde{\kappa}_{DB}^{JK} + T_1^{kjJK} \tilde{\kappa}_{DE}^{JK} + T_1^{jkJK} \tilde{\kappa}_{HB}^{JK}$$
(A3)

where $T_0^{jkJK} = R^{jJ}R^{kK}$ and $T_1^{jkJK} = R^{jP}R^{kJ}\varepsilon^{KPQ}\beta^Q$. Setting all components to zero except for $\tilde{\kappa}_{tr}$ and $\tilde{\kappa}_{0+}$ terms means that (A1) and (A2) become zero as they do not depend on these terms. These time dependencies will modulate the laboratory observable given by (27) at specific frequencies relating to both the boosts and rotations, we calculate these modulations for stationary and rotating experiments in the following sections. However, we only list $\tilde{\kappa}_{0+}$ coefficients that are directly sensitive to the measurement and not suppressed by the boost term, and we do not list the constant terms only the time varying ones. Also, it is noted that all modulations occur around the spin and earth's rotation frequency, and that modulations around twice these values are zero. This is not the case for the established resonator experiments that have put limits on the other parameters ^{15, 39}.

1. Stationary laboratory experiments

Substituting (A3) into (27) and using the same form of rotations and boosts that describe the earths motion with respect to the sun centered celestial equatorial frame, the non-zero coefficients of modulation are given in table 1 to 3. Note that there are no modulation frequencies that directly vary the $\tilde{\kappa}_{0+}^{XY}$ coefficient. This is because the orientation in the sun-centred frame varies only with the rotation of the Earth, and it is this symmetry with respect to the rotation axis, which makes these experiments insensitive to $\tilde{\kappa}_{0+}^{XY}$.

Table I, Sensitivity coefficients of $\beta_0 \tilde{\kappa}_{tr}$ at the relevant modulation frequencies

Modulation	$eta_0 \tilde{\kappa}_{tr}$ Coefficient	
$Cos[\omega_{\oplus}T_{\oplus} + \Omega_{\!\oplus}T]$	$-(1-Cos[\eta])\Big((\mathcal{M}_{DB})_{lab}^{xz}-(\mathcal{M}_{DB})_{lab}^{zx}\Big)$	

$Sin[\omega_{\oplus}T_{\oplus} + \Omega_{\oplus}T]$	$(1 - Cos[\eta]) \left(Cos[\chi] \left(\left(\mathcal{M}_{DB} \right)_{lab}^{yz} - \left(\mathcal{M}_{DB} \right)_{lab}^{zy} \right) + Sin[\chi] \left(\left(\mathcal{M}_{DB} \right)_{lab}^{xy} - \left(\mathcal{M}_{DB} \right)_{lab}^{yx} \right) \right)$	
$Cos[\omega_{\oplus}T_{\oplus} - \Omega_{\oplus}T]$	$(1 + Cos[\eta]) ((\mathcal{M}_{DB})_{lab}^{xz} - (\mathcal{M}_{DB})_{lab}^{zx})$	
$Sin[\omega_{\oplus}T_{\oplus}-\Omega_{\oplus}T]$	$-(1+Cos[\eta])\left(Cos[\chi]\left(\left(\mathcal{M}_{DB}\right)_{lab}^{yz}-\left(\mathcal{M}_{DB}\right)_{lab}^{zy}\right)+Sin[\chi]\left(\left(\mathcal{M}_{DB}\right)_{lab}^{xy}-\left(\mathcal{M}_{DB}\right)_{lab}^{yx}\right)\right)$	

Table II, Sensitivity coefficients of $\tilde{\kappa}^{X\!Z}_{0+}$ at the relevant modulation frequencies

Modulation	$\tilde{\kappa}_{0+}^{XZ}$ Coefficient	
$Cos[\omega_{\oplus}T_{\oplus}]$	$\left(\left(\mathcal{M}_{DB} ight)_{lab}^{\scriptscriptstyle XZ}-\left(\mathcal{M}_{DB} ight)_{lab}^{\scriptscriptstyle ZX} ight)$	
$Sin[\omega_{\oplus}T_{\oplus}]$	$-Cos[\chi]\Big(\big(\mathcal{M}_{DB}\big)_{lab}^{yz} - \big(\mathcal{M}_{DB}\big)_{lab}^{zy}\Big) - Sin[\chi]\Big(\big(\mathcal{M}_{DB}\big)_{lab}^{xy} - \big(\mathcal{M}_{DB}\big)_{lab}^{yx}\Big)$	

Table III, Sensitivity coefficients of $\tilde{\kappa}_{0+}^{YZ}$ at the relevant modulation frequencies

Modulation	$\tilde{\kappa}_{0+}^{YZ}$ Coefficient	
$Cos[\omega_{\oplus}T_{\oplus}]$	$Cos[\chi] \left((\mathcal{M}_{DB})_{lab}^{yz} - (\mathcal{M}_{DB})_{lab}^{zy} \right) + Sin[\chi] \left((\mathcal{M}_{DB})_{lab}^{xy} - (\mathcal{M}_{DB})_{lab}^{yx} \right)$	
$Sin[\omega_{\oplus}T_{\oplus}]$	$\left(\left(\mathcal{M}_{DB}\right)_{lab}^{xz}-\left(\mathcal{M}_{DB}\right)_{lab}^{zx}\right)$	

Here χ is the angle of the colatitude of the experiment from the north-pole of the earth, η is the angle between the celestial equatorial plane and the ecliptic, the path of the Earth's orbital motion (~23.4°), Ω_{\oplus} the angular velocity and speed of the Earth's orbital motion, ω_{\oplus} is the angular velocity of the Earth's rotation, and the times T and T_{\oplus} are the time since a spring equinox and the time since the lab frame y-axis pointed towards 90 ° right ascension.

2. Rotating laboratory experiments

To calculate the dependence of a rotating laboratory experiment, we assume rotation is taken about the z-axis of the laboratory frame at a spin frequency of ω_s . As suggested in Kostelecky and Mewes ¹¹, we transform the \mathcal{M} matrices using a standard tensor rotations in the laboratory frame, so that the components of the \mathcal{M} matrices become time dependent at the spin frequency and twice the spin frequency. Of course the \mathcal{M}^{ZZ} component is the only one to remain unaffected. Also, it should be noted that through the rotation the $\tilde{\kappa}_{0+}^{xy}$ can be directly measured without the boost term suppression. Here we define β_R as the speed of the earth's orbital motion at the equator expressed as a fraction of the speed of light, which is 1.5×10^{-6} , and the time T_S is the time since the rotating experiment's y-axis pointed towards 90 ° right ascension.

Table IV, Sensitivity coefficients of $\beta_0 \tilde{\kappa}_{tr}$ at the relevant modulation frequencies

Modulation $\beta_0 \tilde{\kappa}_{tr}$ Coefficient
--

$Cos[\omega_S T_S]$	$-2\frac{\beta_r}{\beta_0}Sin[\chi]\Big(\big(\mathcal{M}_{DB}\big)_{lab}^{xz}-\big(\mathcal{M}_{DB}\big)_{lab}^{zx}\Big)$
$Sin[\omega_S T_S]$	$-2\frac{\beta_r}{\beta_0}Sin[\chi]\Big(\big(\mathcal{M}_{DB}\big)_{lab}^{yz}-\big(\mathcal{M}_{DB}\big)_{lab}^{zy}\Big)$
$Cos[\omega_S T_S + \Omega_{\oplus} T]$	$Sin[\chi]Sin[\eta]\Big(\Big(\mathcal{M}_{DB}\Big)_{lab}^{yz}-\Big(\mathcal{M}_{DB}\Big)_{lab}^{zy}\Big)$
$Sin[\omega_S T_S + \Omega_{\oplus} T]$	$-Sin[\chi]Sin[\eta]\Big((\mathcal{M}_{DB})_{lab}^{xz}-(\mathcal{M}_{DB})_{lab}^{zx}\Big)$
$Cos[\omega_S T_S - \Omega_{\oplus} T]$	$Sin[\chi]Sin[\eta] \left(\left(\mathcal{M}_{DB} \right)_{lab}^{yz} - \left(\mathcal{M}_{DB} \right)_{lab}^{zy} \right)$
$Sin[\omega_S T_S - \Omega_{\oplus} T]$	$-Sin[\chi]Sin[\eta]\Big((\mathcal{M}_{DB})_{lab}^{xz}-(\mathcal{M}_{DB})_{lab}^{zx}\Big)$
$Cos[\omega_S T_S + \omega_{\oplus} T_{\oplus} + \Omega_{\oplus} T]$	$-\frac{1}{2}(1-Cos[\chi])(1-Cos[\eta])\left(\left(\mathcal{M}_{DB}\right)_{lab}^{xz}-\left(\mathcal{M}_{DB}\right)_{lab}^{zx}\right)$
$Sin[\omega_S T_S + \omega_{\oplus} T_{\oplus} + \Omega_{\oplus} T]$	$-\frac{1}{2}(1-Cos[\chi])(1-Cos[\eta])\left(\left(\mathcal{M}_{DB}\right)_{lab}^{yz}-\left(\mathcal{M}_{DB}\right)_{lab}^{zy}\right)$
$Cos[\omega_S T_S + \omega_{\oplus} T_{\oplus} - \Omega_{\oplus} T]$	$\frac{1}{2}(1 - Cos[\chi])(1 + Cos[\eta])\left(\left(\mathcal{M}_{DB}\right)_{lab}^{xz} - \left(\mathcal{M}_{DB}\right)_{lab}^{zx}\right)$
$Sin[\omega_S T_S + \omega_{\oplus} T_{\oplus} - \Omega_{\oplus} T]$	$\frac{1}{2}(1 - Cos[\chi])(1 + Cos[\eta])\left(\left(\mathcal{M}_{DB}\right)_{lab}^{yz} - \left(\mathcal{M}_{DB}\right)_{lab}^{zy}\right)$
$Cos[\omega_S T_S - \omega_{\oplus} T_{\oplus} + \Omega_{\oplus} T]$	$\frac{1}{2}(1+Cos[\chi])(1+Cos[\eta])\left(\left(\mathcal{M}_{DB}\right)_{lab}^{xz}-\left(\mathcal{M}_{DB}\right)_{lab}^{zx}\right)$
$Sin[\omega_S T_S - \omega_{\oplus} T_{\oplus} + \Omega_{\oplus} T]$	$\frac{1}{2}(1+Cos[\chi])(1+Cos[\eta])\left(\left(\mathcal{M}_{DB}\right)_{lab}^{yz}-\left(\mathcal{M}_{DB}\right)_{lab}^{zy}\right)$
$Cos[\omega_S T_S - \omega_{\oplus} T_{\oplus} - \Omega_{\oplus} T]$	$-\frac{1}{2}(1+Cos[\chi])(1-Cos[\eta])\left(\left(\mathcal{M}_{DB}\right)_{lab}^{xz}-\left(\mathcal{M}_{DB}\right)_{lab}^{zx}\right)$
$Sin[\omega_S T_S - \omega_{\oplus} T_{\oplus} - \Omega_{\oplus} T]$	$-\frac{1}{2}(1+Cos[\chi])(1-Cos[\eta])\left(\left(\mathcal{M}_{DB}\right)_{lab}^{yz}-\left(\mathcal{M}_{DB}\right)_{lab}^{zy}\right)$

Table V, Sensitivity coefficients of $\tilde{\kappa}_{0+}^{xy}$ at the relevant modulation frequencies

	<u> </u>	0+	
Modulation $\tilde{\kappa}_{0+}^{xy}$ Coefficient			
	$Cos[\omega_S T_S]$	$-Sin[\chi]\Big((\mathcal{M}_{DB})_{lab}^{yz}-(\mathcal{M}_{DB})_{lab}^{zy}\Big)$	
	$Sin[\omega_S T_S]$	$Sin[\chi] \Big((\mathcal{M}_{DB})_{lab}^{xz} - (\mathcal{M}_{DB})_{lab}^{zx} \Big)$	

Table VI, Sensitivity coefficients of $\tilde{\kappa}_{0+}^{xz}$ at the relevant modulation frequencies

Modulation	$\tilde{\kappa}_{0+}^{xz}$ Coefficient	
$Cos[\omega_S T_S + \omega_{\oplus} T_{\oplus}]$	$(1 - Cos[\chi]) \left(\left(\mathcal{M}_{DB} \right)_{lab}^{xz} - \left(\mathcal{M}_{DB} \right)_{lab}^{zx} \right)$	
$Sin[\omega_S T_S + \omega_{\oplus} T_{\oplus}]$	$(1 - Cos[\chi]) \left(\left(\mathcal{M}_{DB} \right)_{lab}^{yz} - \left(\mathcal{M}_{DB} \right)_{lab}^{zy} \right)$	
$Cos[\omega_S T_S - \omega_{\oplus} T_{\oplus}]$	$(1 + Cos[\chi]) \left(\left(\mathcal{M}_{DB} \right)_{lab}^{xz} - \left(\mathcal{M}_{DB} \right)_{lab}^{zx} \right)$	
$Sin[\omega_S T_S - \omega_{\oplus} T_{\oplus}]$	$(1 + Cos[\chi]) \left(\left(\mathcal{M}_{DB} \right)_{lab}^{yz} - \left(\mathcal{M}_{DB} \right)_{lab}^{zy} \right)$	

Table VII, Sensitivity coefficients of $\tilde{\kappa}^{yz}_{0+}$ at the relevant modulation frequencies

*	•	01	<u>-</u>
Modulation		$\tilde{\kappa}^{yz}_{0+}$ Coeffic	cient

$Cos[\omega_S T_S + \omega_{\oplus} T_{\oplus}]$	$-(1 - Cos[\chi]) \left(\left(\mathcal{M}_{DB} \right)_{lab}^{yz} - \left(\mathcal{M}_{DB} \right)_{lab}^{zy} \right)$
$Sin[\omega_S T_S + \omega_{\oplus} T_{\oplus}]$	$(1 - Cos[\chi]) \left(\left(\mathcal{M}_{DB} \right)_{lab}^{xz} - \left(\mathcal{M}_{DB} \right)_{lab}^{zx} \right)$
$Cos[\omega_S T_S - \omega_{\oplus} T_{\oplus}]$	$(1 + Cos[\chi]) \left(\left(\mathcal{M}_{DB} \right)_{lab}^{yz} - \left(\mathcal{M}_{DB} \right)_{lab}^{zy} \right)$
$Sin[\omega_S T_S - \omega_{\oplus} T_{\oplus}]$	$-(1+Cos[\chi])\Big(\big(\mathcal{M}_{DB}\big)_{lab}^{xz}-\big(\mathcal{M}_{DB}\big)_{lab}^{zx}\Big)$

APPENDIX B: RECTANGULAR WAVEGUIDE IN THE SME

In this appendix we consider a perfectly conducting rectangular waveguide, filled with isotropic material of relative permittivity and permeability ε_r and μ_r respectively, with height a and width b, oriented along the z-axis in the laboratory frame. The solution of Maxwell's equations using separation of variable gives the following well-known solution for Transverse Electric (TE) modes.

$$E = \left(E_{xo}\hat{x} + E_{yo}\hat{y} + E_{zo}\hat{z}\right)e^{-i\beta z}e^{i\omega t}$$

$$B = \left(B_{xo}\hat{x} + B_{yo}\hat{y} + B_{zo}\hat{z}\right)e^{-i\beta z}e^{i\omega t}$$

$$B_{zo} = B_o \cos[k_x x]\cos[k_y y]$$

$$B_{xo} = B_o \frac{i\beta . k_x}{k^2 - \beta^2}\sin[k_x x]\cos[k_y y]$$

$$B_{yo} = B_o \frac{i\beta . k_y}{k^2 - \beta^2}\cos[k_x x]\sin[k_y y]$$

$$E_{xo} = B_o \frac{i\omega . k_y}{k^2 - \beta^2}\cos[k_x x]\sin[k_y y]$$

$$E_{yo} = B_o \frac{-i\omega . k_x}{k^2 - \beta^2}\sin[k_x x]\cos[k_y y]$$

where $k = \omega \sqrt{\varepsilon_0 \mu_0 \varepsilon_r \mu_r}$, is the free space propagation constant, $k_x = \frac{m\pi}{a}$ and $k_y = \frac{n\pi}{b}$, where n and m are integers greater or equal to zero. To find the phase shift over length L due to leading order Lorentz violating terms in the SME we compute the \mathcal{M} matrices given by (27), and find the following non-zero components;

$$(\mathcal{M}_{DE})_{lab}^{xx} = \frac{\pi L}{\lambda_{v}} \left(\frac{k_{y}^{2}}{k_{x}^{2} + k_{y}^{2}} \right) \frac{v_{ph}}{c} \mu_{r}$$

$$(\mathcal{M}_{DE})_{lab}^{yy} = \frac{\pi L}{\lambda_{v}} \left(\frac{k_{x}^{2}}{k_{x}^{2} + k_{y}^{2}} \right) \frac{v_{ph}}{c} \mu_{r}$$

$$(\mathcal{M}_{HB})_{lab}^{xx} = -\frac{\pi L}{\lambda_{v}} \left(\frac{k_{x}^{2}}{k_{x}^{2} + k_{y}^{2}} \right) \frac{c}{v_{ph}} \mu_{r}$$

$$(\mathcal{M}_{HB})_{lab}^{xx} = -\frac{\pi L}{\lambda_{v}} \left(\frac{k_{x}^{2}}{k_{x}^{2} + k_{y}^{2}} \right) \frac{c}{v_{ph}} \mu_{r}$$

$$\begin{split} \left(\mathcal{M}_{HB}\right)_{lab}^{yy} &= -\frac{\pi L}{\lambda_{v}} \left(\frac{k_{y}^{2}}{k_{x}^{2} + k_{y}^{2}}\right) \frac{c}{v_{ph}} \mu_{r} \\ \left(\mathcal{M}_{HB}\right)_{lab}^{zz} &= -\frac{\pi L}{\lambda_{v}} \left(\frac{k_{x}^{2} + k_{y}^{2}}{k_{0}^{2}}\right) \frac{v_{ph}}{c} \mu_{r} \\ \left(\mathcal{M}_{DB}\right)_{lab}^{xy} &= \frac{2\pi L}{\lambda_{v}} \left(\frac{k_{y}^{2}}{k_{x}^{2} + k_{y}^{2}}\right) \mu_{r} \\ \left(\mathcal{M}_{DB}\right)_{lab}^{yx} &= -\frac{2\pi L}{\lambda_{v}} \left(\frac{k_{x}^{2}}{k_{x}^{2} + k_{y}^{2}}\right) \mu_{r} \\ v_{ph} &= \frac{\omega}{\sqrt{k^{2} - k_{y}^{2} - k_{y}^{2}}} \end{split}$$

Here, v_{ph} is the phase velocity of the mode inside the waveguide. These values reduce to those calculated for the plane wave in the appropriate limits. By letting a and then b tend to infinity we recover the (x, y) polarization as in equation (17) and vice versa for the (y, x) polarization (18). It should be noted that;

$$\left(\mathcal{M}_{DB}\right)_{lab}^{xy} - \left(\mathcal{M}_{DB}\right)_{lab}^{yx} = \frac{2\pi L}{\lambda_{y}} \mu_{r}$$
 (B3)

is independent of k_x and k_y , and is the same as the plane wave case. Because equation (B3) is non-zero, the propagation of the mode will depend on the $\tilde{\kappa}_{tr}$ and $\tilde{\kappa}_{0+}$ coefficients in the sun-centered celestial equatorial frame as shown in Appendix A. Furthermore, the sensitivity is independent of mode of propagation in the waveguide.

References

- 1 C. M. Will, *Theory and Experiment in Gravitational Physics, revised edition* (Cambridge University Press, Cambridge, 1993).
- ² A. Kostelecky and S. Samuel, Phys. Rev. D. 39, 683 (1989).
- 3 T. Damour, gr-qc/9711060.
- 4 R. Gambini and J. Pullin, Phys. Rev D. 39 (1999).
- ⁵ H. P. Robertson, Rev. Mod. Phys. 21, 378-382 (1949).
- 6 R. Mansouri and R. U. Sexl, Gen. Relativ. Gravit. 8, 497-514 (1977).
- ⁷ A. P. Lightman and D. L. Lee, Phys. rev. D 8, 364 (1973).
- 8 D. Colladay and A. Kostelecky, Phys. Rev. D. 55, 6760-6774 (1997).
- ⁹ D. Colladay and A. Kostelecky, Phys. Rev. D. 58 116002 (1998).
- 10 A. Kostelecky, Phys. Rev. D. 69, 105009 (2004).
- 11 A. Kostelecky and M. Mewes, Phys. Rev. D 66, 056005 (2002).
- ¹² A. Kostelecky and M. Mewes, Phys. Rev. Lett. 87 251304 (2001).
- ¹³ J. A. Lipa, J. A. Nissen, S. Wang, *et al.*, Phys. Rev. Lett. 90, 060403 (2003).
- H. Muller, S. Herrmann, C. Braxmaier, et al., Phys. Rev. Lett 91 (2003).

- 15 P. Wolf, S. Bize, A. Clairon, *et al.*, Accepted; Phys. Rev. D rapid comm. arXiv:hep-ph/0407232 (2004).
- 16 H. Muller, S. Herrmann, A. Saenz, et al., Phys. Rev. D. 68, 116006 (2003).
- 17 P. Wolf, S. Bize, A. Clairon, et al., Phys. Rev. Let. 90 (2003).
- ¹⁸ M. E. Tobar, J. G. Hartnett, and J. D. Anstie, Phys. Lett. A. vol. 300/1 (2002).
- ¹⁹ A. A. Michelson and E. W. Morley, Am. J. Sci. 34, 333 (1887).
- ²⁰ J. J. Kennedy and E. M. Thorndike, Phys. Rev. B 42, 400 (1932).
- ²¹ H. E. Ives and G. R. Stilwell, J. Opt. Soc. Am. 28, 215 (1938).
- 22 G. Saathoff, S. Karpuk, U. Eisenbarth, et al., Phys. Rev. Lett 91 (2003).
- 23 K. C. Turner and H. A. Hill, Phys. Rev. 134, 252 (1964).
- ²⁴ E. Riis, L. Andersen, N. Bjerre, *et al.*, Phys. Rev. Lett. 60, 81-84 (1988).
- ²⁵ R. Grieser and etal, Appl. Phys. B 59, 127 (1994).
- ²⁶ T. P. Krisher, L. Maleki, G. F. Lutes, et al., Phys. Rev. D 42, 731-734 (1990).
- ²⁷ P. Wolf and G. Petit, Phys. Rev. A 56, 4405-4409 (1997).
- ²⁸ P. Wolf, Phys. rev. A 51, 5016-5018 (1995).
- ²⁹ Q. G. Bailey and V. A. Kostelecky, arXiv: hep-ph/0407252 (2004).
- 30 E. N. Ivanov, M. E. Tobar, and R. A. Woode, IEEE Trans. on UFFC 45, 1526-1536 (1998).
- 31 E. N. Ivanov and M. E. Tobar, IEEE Trans. Ferroelect. Freq. Contr. 49, 1160-1165 (2003).
- P. R. Saulson, Fundamentals of Interferometric Gravitational Wave Detectors (World Scientific, 1994).
- 33 A. G. Gurevich, *Ferrites at Microwave Frequencies* (State Press for Physicomathematical Literature, Moscow, 1960).
- 34 E. N. Ivanov, M. E. Tobar, and R. A. Woode, IEEE Trans. on Micrw. Theory Tech. 46, 1537-45 (1998).
- J. Krupka and R. Geyer, IEEE Trans. Microw. Theory Techn. 32, 1924-1933 (1996).
- 36 M. R. F. Jensen, S. A. Feiven, T. J. Parker, et al., Phys. Rev. B 55, 2745-2748 (1997).
- ³⁷ A. D. Karsono and D. R. Tilley, J. Phys. C: Solid State Phys. 11, 277-289 (1978).
- 38 K. Abraha and D. R. Tilley, Surface Science Reports 24, 129-222 (1996).
- ³⁹ P. Wolf, M. E. Tobar, S. Bize, *et al.*, Gen. Rel. Grav. 36 (2004).
- 40 A. Kostelecky, private communication, 30/7/2004.